Macromolecular crowding impacts on the diffusion and conformation of DNA hairpins

Olivia Stiehl, Kathrin Weidner-Hertrampf, and Matthias Weiss*
Experimental Physics I, University of Bayreuth, Universitätsstrasse 30, D-95440 Bayreuth, Germany
(Received 14 July 2014; revised manuscript received 27 October 2014; published 12 January 2015)

Biochemical reactions in crowded fluids differ significantly from those in dilute solutions. Both, excluded-volume interactions with surrounding macromolecules ("crowders") and an enhanced rebinding of reaction partners due to crowding-induced viscoelasticity and subdiffusion have been hypothesized to shift chemical equilibria towards the associated state. We have explored the impact of both cues in an experimentally tunable system by monitoring the steady-state fraction of open DNA hairpins in crowded fluids with varying viscoelastic characteristics but similar occupied volume fractions. As a result, we observed an increased fraction of closed DNA hairpins in viscoelastic crowded fluids. Our observations compare favorably to a simple statistical model that considers both facets of crowding, while preferential interactions between crowders and DNA hairpins appear to have little influence.

DOI: 10.1103/PhysRevE.91.012703 PACS number(s): 87.15.Vv, 05.40.Jc, 87.15.Ya, 82.33.Ln

I. INTRODUCTION

Cellular fluids like the cytoplasm are crowded with a plethora of macromolecules at a total concentration of up to 400 mg/ml [1]. Owing to the associated excluded volume, the presence of "crowders" has been predicted to enhance protein folding, complex formation, and membrane association (see, for example, Ref. [2] for a comprehensive review). Indeed, several simulation studies and experimental reports have given support to this notion albeit subtle details due to the chemical nature of the crowding agents have led to nonuniform interpretations [2]. Besides a change in equilibrium properties of (bio)chemical reactions, the impact of crowding on the diffusion of macromolecules has also been discussed extensively. Crowded fluids not only feature a significantly slower diffusion [3] but also an anomalous diffusion ("subdiffusion") has been reported in several instances [4–9] (see [10] for a recent and comprehensive overview).

Subdiffusion is characterized by a nonlinear scaling of the particles' mean square displacement (MSD), $\langle r(t)^2\rangle \sim t^\alpha$ with $\alpha < 1$. Interestingly, the scaling of the ensemble-averaged and time-averaged MSD can be different if the underlying random walk shows a weak ergodicity breaking [11,12]. Recent experimental data, however, have provided strong evidence that crowded fluids are viscoelastic on certain scales [13,14] which is reflected in a subdiffusive fractional Brownian motion of tracer macromolecules on short and intermediate time scales [15–18]. As a consequence, biochemical reactions have been predicted to differ strongly from those in purely viscous solutions [19–21]. In line with this, we recently have been able to show that the opening and closing kinetics of a single-stranded DNA hairpin not only is slowed down by crowding-induced subdiffusion. Rather, also the closed state of the hairpin was significantly favored in crowded fluids that feature an anomalous diffusion [22]. However, in this study the fluid's viscoelastic properties (reflected in the diffusion anomaly) could be varied only by changing the type of crowder. Therefore, a detailed investigation of the differential effects of excluded-volume interactions and viscoelasticity of the crowded fluid had not been possible.

Here, we have combined fluorescence correlation spectroscopy (FCS) and UV absorption spectroscopy to explore the impact of these two facets of crowding on the steady state of a (bio)chemical reaction. In particular, we have evaluated the viscoelasticity of several crowded fluids via the diffusional motion of macromolecules ("passive microrheology") and monitored subsequently the fraction of open DNA hairpins in these fluids. As a result, we observed that an addition of macromolecular crowders increases the fraction of closed DNA hairpins as compared to low-weight additives like sucrose. This effect is even enhanced when the fluid also has viscoelastic characteristics and therefore features a subdiffusive motion of the hairpins. Our observations are in favorable agreement with a simple statistical model that considers both facets of crowding while preferential interactions between crowders and hairpins appear to have little influence.

II. MATERIALS AND METHODS

A. Chemicals

Crowding agents (sucrose from Roth; 10 kDa polyethylene glycol (PEG) and 10 kDa dextran from Sigma) were dissolved either in MilliQ water or TE buffer [1 mM ethylene diamine tetra-acetic acid (EDTA), 100 mM NaCl, 10 mM tris(hydroxymethyl)aminomethane (Tris) at pH 7.5] in accordance with [23]. All additives were used at 10% and 30% weight per volume.

For UV spectroscopy, three single-stranded DNA (ssDNA) constructs with the same stem region but different loop lengths were used (metabion, Planegg-Martinsried, Germany): C_3A_2-X-T_2G_3 with $X = T_{21}, T_{30}, T_{50}$. For fluoresence correlation spectroscopy we have used as tracers (i) 10 kDa dextran (coupled to Alexa 488; Lifetechnologies, Carlsbad, CA), and (ii) single-stranded DNA C_3A_2-T_{21}-T_2G_3 (coupled to the rhodamine derivative FAM; GenScript Inc., Piscataway, NJ).

B. Fluorescence correlation spectroscopy

FCS experiments were performed at room temperature on a Leica SP5-TCSPC system (Leica Microsystems, Mannheim,

*Author to whom correspondence should be addressed: matthias.weiss@uni-bayreuth.de

Germany and Picoquant, Berlin, Germany) with a 63×, 1.2 numerical aperture water immersion objective. Tracer particles were excited at 470 nm with a pulsed laser; the detection bandpass was set to 500–550 nm.

Data acquisition for FCS routinely was limited to 60 s; DNA data were occasionally recorded for 120 s due to a low quantum yield of the FAM dye. Correlation curves were fitted with MATLAB using a previously established fitting function for anomalous diffusion in bulk fluids [4,15]:

$$C_D(\tau) = \frac{\mathcal{A}}{[1+(\tau/\tau_D)^{\alpha}]\sqrt{1+q(\tau/\tau_D)^{\alpha}}}. \quad (1)$$

Here, α denotes the potential diffusion anomaly, and τ_D is the mean dwell time of a fluorescent particle within the confocal volume. The prefactor $\mathcal{A}$ summarizes the inverse number of particles within the confocal volume and photophysics of the fluorophores. Since data evaluation was restricted to times $\tau > 30\ \mu$s, the contribution of the photophysics was negligible and therefore was not taken into account explicitly.

We would like to note that normal diffusion ($\alpha = 1$) is trivially included in Eq. (1), and in this case the mean dwell time is determined by the radius of the confocal volume r_0 and the diffusion constant D of the tracer particle: $\tau_D = r_0^2/(4D)$. The diffusion constant is given by the Einstein-Stokes equation $D = k_B T/(6\pi\eta R_H)$ with $k_B T$ and η denoting the thermal energy and the fluid's viscosity, respectively; R_H denotes the tracer's hydrodynamic radius. Elongation of the confocal volume along the optical axis is considered in Eq. (1) via the parameter q which was fixed to $q = 0.04$ throughout the evaluation process. Mean values reported here for α and τ_D are based on at least 40 FCS curves taken on three different days.

C. UV spectroscopy

UV-absorption measurements were performed on a Specord 250 Plus (Analytik Jena, Jena, Germany), equipped with a temperature-stabilized sample holder. The sample holder accomodated two cuvettes (for fluids with and without DNA constructs) that were addressed by two independent UV beams. The instrument hence provided a direct readout of the background-corrected DNA hyperchromicity as a function of temperature (enhanced UV absorption upon temperature-induced loss of base pairing). Since DNA hyperchromicity is routinely detected for illumination wavelengths of 250–270 nm [24], we have recorded UV absorption spectra from 200 to 320 nm as a function of temperature. Temperature was varied from 0 °C to 90 °C in steps of 1 °C. After a temperature shift the sample was allowed to equilibrate for 30 s. Depending on the DNA sequence, the maximum temperature of the scan was reduced if possible.

Evaluation of the spectra was performed with MATLAB. To this end, the mean absorption in the range 250–270 nm was plotted as a function of temperature. We manually determined the temperature at which the curve saturates (vanishing slope). The corresponding absorption level A_{open} reflects an ensemble where (almost) all ssDNA strands are open. To extract the probability of being open at room temperature (at which we have performed our FCS experiments), we divided the absorption value at 20 °C, A_{20}, by A_{open}. The fraction of open hairpins, $p = A_{20}/A_{\text{open}}$, obtained in this way reflects a single DNA molecule's probability of being in the open state at room temperature. This approach was applied to each of the three ssDNA contructs in TE buffer containing dextran (10 kDa), PEG (10 kDa), or sucrose as crowders. Reading off A_{open} and A_{20} in several experiments and evaluation rounds yielded a maximum uncertainty in p of ± 0.06. We therefore have used this upper bound for error bars shown in Fig. 4.

III. RESULTS AND DISCUSSION

A. Establishing crowded fluids with varying viscoelasticity

In order to explore the impact of a crowded fluid's viscoelastic nature on (bio)chemical reactions, we first sought to establish crowded fluids with varying material properties at similar occupied-volume fractions. To this end, we monitored the diffusional motion of two fluorescently tagged tracer particles (10 kDa dextran, and a $C_3A_2T_{23}G_3$ ssDNA construct) in several crowded fluids by means of fluorescence correlation spectroscopy (see the Materials and Methods section for details). Indeed, monitoring the MSD of nanoparticles, for example by FCS, allows one to draw conclusions on the viscoelastic properties of the fluid on small scales (passive microrheology) [13,25]. In particular, a subdiffusive scaling of the MSD [$\langle r(t)^2\rangle \sim t^{\alpha}$ with $\alpha < 1$] indicates the emergence of an elastic contribution in the complex shear modulus $G(\omega)$, hence reporting on a fluid's viscoelastic characteristics. As a matter of fact, passive microrheology is widely applied [26] and has revealed that dextran-crowded aqueous fuids are viscoelastic on small length and time scales, hence featuring a subdiffusive fractional Brownian motion of tracer particles ($\alpha \approx 0.8$) [16,17]; in contrast, dense sucrose solutions appeared purely viscous ($\alpha \approx 1$).

Dextran, a branched oligosaccharide, is a well-established, biocompatible crowding agent [2] that is capable of rendering a fluid viscoelastic when dissolved in water at high concentrations [16,17]. We therefore focused on this compound as crowding agent. Crowded fluids were hence made up of unlabeled 10 kDa dextran (100 g/l and 300 g/l) dissolved in either MilliQ water or TE buffer (see the Materials and Methods section for details). Representative FCS curves of the above-mentioned tracer particles in these different host fluids are shown in Fig. 1. From these we extracted the typical dwell time of particles in the focal volume, τ_D, and the diffusion anomaly α.

In agreement with previous reports [4,6,15], we observed that both fluorescent tracers showed a subdiffusive autocorrelation decay in dextran-crowded fluids based on water as a solvent (Fig. 2), indicating a significant viscoelasticity of the fluid. In contrast, dextran-crowded fluids based on TE buffer appeared purely viscous as they showed a significantly weaker diffusion anomaly (Fig. 2). As anticipated, sucrose solutions showed no significant diffusion anomaly, i.e., no viscoelasticity, irrespective of the solvent (on average $\alpha \approx 0.95$; Fig. 3). Slight deviations of α from unity for viscous fluids most likely are due to minor optical effects [27]. In contrast to α, we did not observe major changes in the time scale of the autocorrelation decay τ_D for any of the crowded fluids when changing the solvent from MilliQ water to TE buffer (Fig. 3). Alteration in the slope of the autocorrelation

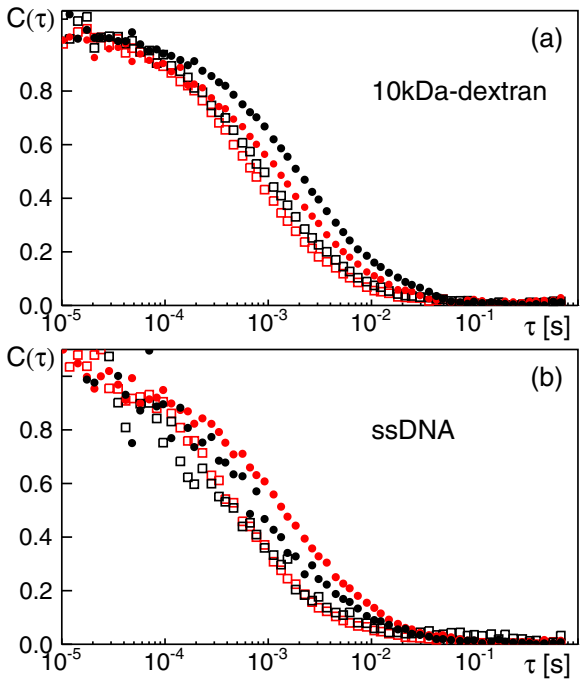

FIG. 1. (Color online) (a) Representative autocorrelation curves $C(\tau)$ of fluorescent 10 kDa dextran tracers immersed in water (black symbols) or TE buffer (red symbols) to which 30% sucrose (open squares) or 30% 10 kDa dextran (filled circles) has been added. Adding dextran crowders significantly shifts the autocorrelation decay to larger time scales. Moreover, the autocorrelation decay is seen to be steeper when using TE buffer instead of water (cf. also Fig. 2). (b) As before for a fluorescently tagged ssDNA (T_{21} loop). Also in this case, using dextran crowders and/or TE buffer instead of water affects the tracer's diffusional behavior.

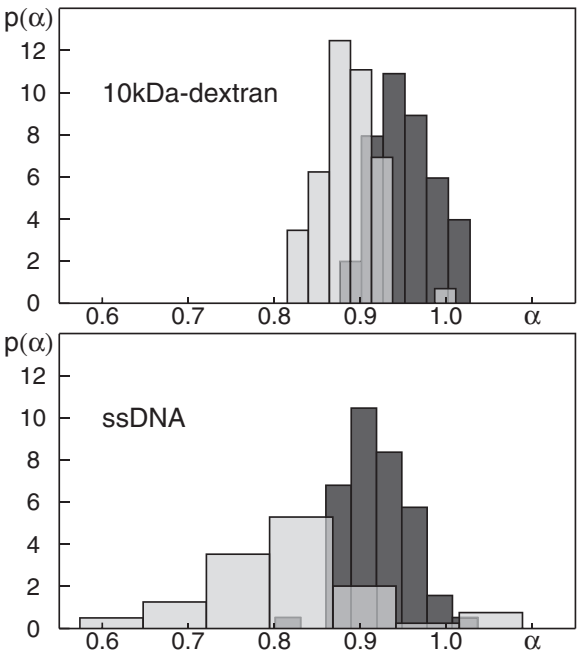

FIG. 2. Probability distributions $p(\alpha)$ for the indicated fluorescent tracers in dextran-crowded fluids (concentration 30%) are significantly different when using MilliQ water (light gray bars) or TE buffer (dark gray bars) as a solvent. A Student's t test revealed a significance level of $<10^{-5}$ between data obtained in MilliQ and TE buffer, and data were consistent with normal distributions according to χ^2 and Jarque-Bera tests (significance level 1%). Thus, a strong difference in the tracers' diffusion anomaly and therefore in the fluids' material properties is observed when changing solvents from water to TE buffer.

decay (determined by α) but not the overall time scale τ_D indicates a similar volume occupancy of dextran in water and TE buffer but different viscoelastic characteristics.

We next aimed at rationalizing the phenomenon that the material properties of dextran-crowded fluids depend on the solvent. Given that TE buffer, unlike MilliQ water, provides a considerable amount of ions, we hypothesized that dextran molecules assume a more compact configuration in TE buffer due to interactions with ions. Therefore, viscoelasticity and subdiffusion would subside in TE buffer due to reduced entanglement of dextran molecules. To probe this hypothesis, we monitored the diffusion of fluorescently tagged dextran at dilute conditions in MilliQ water and TE buffer. From the diffusion time we derived the apparent hydrodynamic radius R_H which reports on the molecule's compactness. We note at this point that performing similar measurements at semidilute conditions may become inaccessible to a quantitative interpretation: In the case of subdiffusion, a meaningful diffusion constant cannot be defined any more, i.e., estimating hydrodynamic radii via the Einstein-Stokes equation fails.

The result of our measurements confirmed the above reasoning, i.e., dextran was indeed slightly more compact in TE buffer as compared to water: The ratio of diffusion times (based on 15 individual FCS measurements per solvent) was $\tau_D^{\mathrm{TE}}/\tau_D^{\mathrm{water}} = (215 \pm 2\ \mu\mathrm{s})/(277 \pm 3\ \mu\mathrm{s}) \approx 0.78$. Since FCS diffusion times are determined via the Einstein-Stokes relation as $\tau_D = 3\pi\eta R_H r_0^2/(2k_BT)$, this experimental result indicates a 20% reduction in dextran's hydrodynamic radius R_H in TE buffer as compared to water. Here, the viscosities of water and TE buffer were assumed to be the same within 1%–2%, which is a reasonable assumption since the major difference between TE buffer and pure water is the presence of ions. Given this significant, yet subtle, change in dextran's hydrodynamic radius, it is conceivable that the occupied volume of semidilute dextran fluids is similar for both solvents while the "surface roughness" needed for entanglement is strongly reduced in TE buffer.

B. DNA hairpin conformation in crowded fluids with varying viscoelasticity

Having established crowded dextran fluids with similar occupied-volume fractions but varying material properties, we next employed these fluids to explore changes of (bio)chemical reactions in crowded fluids. To this end, we considered the stochastic opening and closing of a DNA hairpin with a poly-T loop and five cognate bases in the stem region as a model system (cf. the Materials and Methods section). We had observed previously that an increasing concentration of PEG and dextran crowders dissolved in MilliQ water not only led to a slower kinetics of the opening and closing processes but also significantly affected the steady-state probability of the hairpin

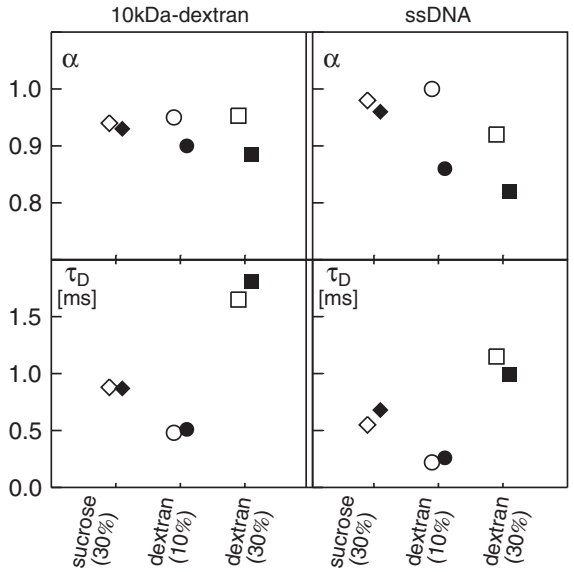

FIG. 3. Summary of mean anomalies (α, top panel) and diffusion times (τ_D, bottom panel) obtained for fluorescent dextran tracer particles (left) and a fluorescently labeled ssDNA (right). Fluids based on MilliQ water (closed sysmbols) and TE buffer (open symbols) contained the amount of sucrose or dextran indicated on the horizontal axis. While α decreased for increasing amounts of dextran crowders in MilliQ water, much less variation in α was observed for the same amounts of dextran crowders in TE buffer. In contrast, values for τ_D hardly depended on the type of solvent but only reflected increasing amounts of dissolved additives (sucrose or dextran). For better visibility, open (closed) symbols have been shifted slightly to the left (right). Please note: Error bars (standard deviation of the mean) are smaller than the symbol size.

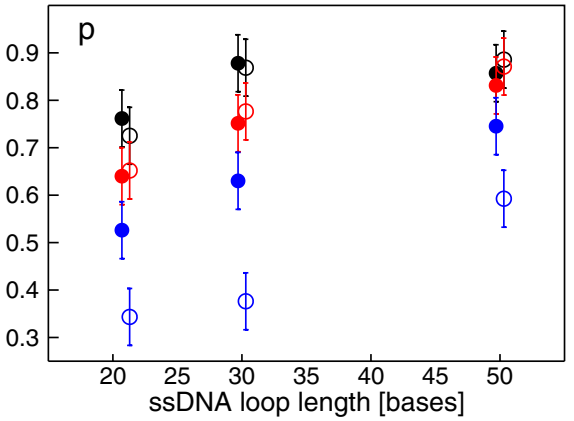

FIG. 4. (Color online) Apparent fraction of open DNA hairpins, p, in crowded TE buffers as quantified via UV absorption experiments (see Materials and Methods section for details). Data for 10% and 30% solutions are shown as filled and open symbols, respectively. Sucrose, dextran, and PEG additions are indicated by colors black, red, and blue (blue symbols have the lowest values of p). For better visibility, data have been shifted by 0.3 to the left (10%) and to the right (30%); error bars represent the uncertainty of determining p as discussed in the Materials and Methods section. While the fraction of open hairpins hardly changes with increasing concentration of sucrose and dextran for three DNA constructs with different loop lengths, PEG shows a pronounced effect. See the main text for further discussion.

to be in the open configuration [22]. This was in strong contrast to dense sucrose solutions where the hairpin's steady-state probability of being in the open state was unaffected. In fact, at the same occupied-volume fraction ϕ, a stronger reduction of open DNA hairpins was observed in dextran-crowded fluids as compared to PEG-crowded fluids (see Table I). These data suggested that crowded fluids with viscoelastic characteristics (dextran in MilliQ water) enhance the probability for DNA hairpins to be in the closed state, whereas the effect is less strong in crowded fluids without a significant viscoelasticity (PEG in MilliQ water).

To explore this point in more detail, we considered PEG and dextran as crowding agents and probed the conformation of several DNA hairpins in TE buffer at different crowder concentrations via UV hyperchromicity (see the Materials and Methods section for details). In fact, a decrease in UV absorption upon base pairing (a closed hairpin) around a wavelength $\lambda \approx 260$ nm is routinely used to assess the structural conformation of DNA [24] due to the attractive pricing of oligonucleotides without a fluoerscence label.

As a result of our UV absorption experiments, we observed a significant reduction in the apparent fraction of open DNA hairpins, p, when the concentration of PEG was increased from 10% to 30% (Fig. 4). Depending on the hairpin's loop length, we observed a reduction of p by factors 0.65 ($T21$ loop), 0.60 ($T30$ loop), and 0.80 ($T50$ loop). In contrast, the amount of open DNA hairpins did not change significantly in dextran-crowded TE buffer nor in sucrose solutions, when the crowder's concentration was increased (Fig. 4).

Seemingly counterintuitive at first glance, these results indeed are in favorable agreement with our hypothesis that crowding impacts the hairpin conformation via two routes: (i) via excluded-volume interactions, and (ii) via rendering the fluid viscoelastic:

(a) Sucrose is a small additive that neither contributes a significant excluded volume nor renders a fluid viscoelastic [17]. Hence, a change in p is neither expected nor observed in dense sucrose fluids (cf. Fig. 4 and Ref. [22]).

(b) PEG-crowded fluids feature a change in p but do not show a significant subdiffusion of tracer particles [22], i.e., PEG-crowded fluids have no viscoelastic characteristics on small length scales. Therefore, the effects of PEG can be attributed solely to excluded-volume interactions. Based on our previously published data (Table I) obtained with fluorescent oligonucleotides, we predict a roughly linear dependence between the hairpin's probability of being in the open state and

TABLE I. Average occupied-volume fraction ϕ and average open probability p of the DNA hairpin as reported in [22]. Data were obtained for crowded fluids based on MilliQ water (weight percentages of dextran and PEG crowders as indicated).

	10%	20%	30%	40%
Dextran	$\phi = 0.035$	$\phi = 0.070$	$\phi = 0.105$	$\phi = 0.141$
	$p = 0.386$	$p = 0.311$	$p = 0.278$	$p = 0.201$
PEG	$\phi = 0.132$	$\phi = 0.265$	$\phi = 0.397$	$\phi = 0.529$
	$p = 0.422$	$p = 0.372$	$p = 0.383$	$p = 0.231$

PEG's volume occupancy: $p(\phi) = 0.492 - 0.425\phi$. Changing the concentration of PEG from 10% to 30% hence should lead to reduction of open hairpins by a factor $p(\phi_{30})/p(\phi_{10}) \approx 0.74$. This prediction compares favorably to our experimental findings (factors 0.65, 0.60, and 0.80 for $T21$, $T30$, and $T50$ loops; Fig. 4).

(c) Using dextran as a crowding agent, and assuming that it also interacts with the hairpin solely via the excluded volume (like PEG), the above linear relation $p(\phi)$ predicts a change in the amount of open hairpins by a factor $p(\phi_{30})/p(\phi_{10}) \approx 0.93$ (values for ϕ taken from Table I). This prediction is in good agreement with our experimental observations for hairpins immersed in dextran-crowded TE buffer (Fig. 4): The amount of open DNA hairpins hardly changed in dextran-crowded TE buffer which lacks viscoelastic characteristics (see the previous section), i.e., dextran provides only excluded-volume interactions. In contrast to this, we previously saw a very strong reduction of p for hairpins in dextran-crowded MilliQ water (Table I) for which we found significant viscoelastic characteristics [22]).

Thus, our findings support the notion that crowded viscoelastic fluids lead to a stronger reduction of the steady-state fraction of open DNA hairpins as compared to fluids that feature mere excluded-volume interactions.

C. Relative importance of crowding contributions

Having seen that crowded fluids affect the steady-state fraction of open DNA hairpins, we aimed at putting this effect into context via a simple statistical model. For simplicity we consider the two ends of the hairpin as individual particles that can occupy any location in a limited volume that is dissected into $\Omega + 1$ lattice sites. Restricting the available space accounts for the polymeric constraint that links both particles. If we fix the position of one of the particles as the point of origin for the lattice, Ω lattice sites are available for the second particle if it is unbound. The bound state is reflected by both particles occupying the point of origin. Denoting the energies associated with the dissociated and associated states by E_S and E_B, the canonical partition function of the system reads

$$Z = \Omega \exp\left(-\frac{E_S}{k_B T}\right) + \exp\left(-\frac{E_B}{k_B T}\right). \tag{2}$$

The steady-state probability of being in the bound state (a closed hairpin) therefore is given by

$$w = \frac{1}{1 + \Omega \exp\left(-\frac{\Delta E}{k_B T}\right)}, \quad \Delta E = E_S - E_B, \tag{3}$$

and the open state's probability is hence $p = 1 - w$.

Introducing a crowding agent like PEG or dextran may affect either the multiplicity of states, i.e., Ω, or the energy difference ΔE. Excluded volume may be considered by invoking the occupied-volume fraction for each site, i.e., $\Omega = (1 - \phi)\Omega_0$. Increasing the occupied-volume fraction via enhanced crowder concentrations decreases Ω, and therefore the hairpin's probability to be in the open state, p, also decreases. This result is in agreement with previous considerations [28].

If crowding also introduces viscoelastic characteristics, the elastic deformation energy stored in the fluid contributes an energy penalty for the unbound state. Thus, ΔE increases and so does w. Thus, the fraction of open hairpins p decreases in agreement with our experimental observations. However, attractive interactions between crowding agents and the hairpin may also increase ΔE. Discriminating this from viscoelasticity-induced effects is experimentally difficult as the two can hardly be tuned independently. Yet relating our results to data in the literature indicates that these attractive interactions may be negligible in our case: First, it has been shown that glucose (the monomer of dextran) and sucrose have only negligible impact on hairpin closure [29]. Moreover, larger crowders in the kDa range (e.g., PEG and dextran crowders) have been shown to contribute only very small attractive interactions to DNA base pairing [29–31]. It is therefore unlikely that a polymeric glucose, i.e., dextran, features a more pronounced attractive interaction with DNA than its individual monomers. Based on this, we conclude that specific interactions between DNA and crowders appear to be negligible for the systems studied here, i.e., all effects seem to be well captured by excluded-volume interactions and crowding-induced viscoelasticity.

Based on this reasoning it appears justified to express ΔE as the sum of a trivial constant and a viscoelasticity-dependent contribution, $\Delta E = \Delta E_0 + \varepsilon(\phi)$. For crowded dextran fluids that feature viscoelasticity and subdiffusion, $\varepsilon(\phi)$ may be estimated as follows: The anomalous mean square displacement $\langle r(t)^2 \rangle \sim t^\alpha$ of a particle performing fractional Browian motion can be transformed into a complex shear modulus of the surrounding fluid [13,25], yielding an elastic modulus

$$G'(\omega) \sim \frac{\omega^\alpha}{\Gamma(\alpha + 1)} \sin\frac{\pi(1 - \alpha)}{2}.$$

Associated with this modulus is a typical deformation energy $\varepsilon(\alpha) = \varepsilon_0 \sin[\pi(1 - \alpha)/2]/\Gamma(\alpha + 1)$ that gives rise to the non-Markovian character of the anomalous random walk. For $\alpha \geqslant 0.6$, this expression can be approximated within 3% accuracy as $\varepsilon(\alpha) \approx 1.65\varepsilon_0(1 - \alpha)$. In addition, an approximately linear relation $\alpha \approx 1 - 2\phi$ has been found experimentally for the diffusion of tracer particles in crowded dextran fluids [4,22]. Therefore, the elastic energy penalty is $\varepsilon(\phi) = 3.3\varepsilon_0\phi$. Inserting this result into Eq. (3) and also considering the entropy-associated term $\Omega = \Omega_0(1 - \phi)$ for mere excluded volume, the fraction of open hairpins reads

$$p = \frac{c_0(1 - \phi)\exp\left(-\frac{3.3\varepsilon_0\phi}{k_B T}\right)}{1 + c_0(1 - \phi)\exp\left(-\frac{3.3\varepsilon_0\phi}{k_B T}\right)} \tag{4}$$

with $c_0 = \Omega_0 \exp(-\Delta E_0/k_B T)$. For fluids without viscoelasticity, i.e., without noticeable subdiffusion, $\varepsilon_0 = 0$. By definition, c_0 and ε_0 are system-specific constants that need to be determined via a comparison of Eq. (4) with experimental data. In our case, the fraction of open hairpins at vanishing crowding conditions ($p \approx 50\%$ at $\phi = 0$) is well captured with $c_0 = 0.9$. Moreover, for PEG-crowded fluids no viscoelasticity needs to be considered, i.e., $\varepsilon_0 = 0$. With this parameter choice, Eq. (4) indeed provides a surprisingly good description of our experimental data for DNA hairpins in PEG-crowded fluids (Fig. 5). Furthermore, Eq. (4) also matches our experimental

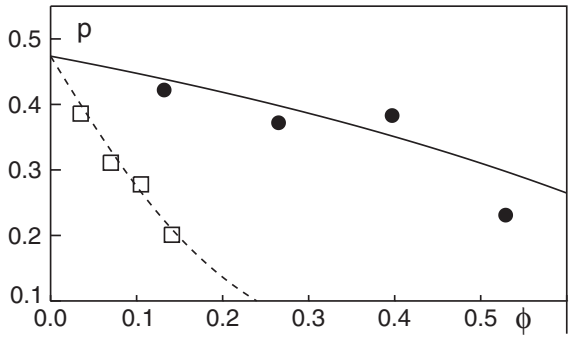

FIG. 5. Fraction of open DNA hairpins (T 21 loop) p as a function of the occupied-volume fraction ϕ in MilliQ water crowded with PEG (filled circles) and dextran (open squares); data taken from Table I. Theoretical estimates based on Eq. (4) for crowded fluids with and without viscoelasticity (dashed and full lines, respectively) are in good agreement with experimental data. Please note: For viscoelastic dextran-crowded fluids, the diffusion anomaly is empirically well captured by $\alpha \approx 1 - 2\phi$. See the main text for details.

data for hairpins in MilliQ water crowded with dextran when leaving $c_0 = 0.9$ unchanged and assuming a modest elastic penalty $\varepsilon_0 = 2.3 k_B T$ to account for the viscoelastic character of the fluid (Fig. 5). As discussed already above, our UV absorption data for hairpins in crowded TE buffer follow the trend for PEG-crowded fluids due to a lack of viscoelasticity, i.e., these data also are in agreement with our theoretical estimate at $\varepsilon_0 = 0$. We therefore conclude that Eq. (4) and the associated reasoning faithfully reflect the essential lines of impact that crowding imposes on the conformational kinetics of DNA hairpins.

IV. CONCLUSIONS

In summary, we have experimentally explored the impact of excluded volume and crowding-induced viscoelasticity on a typical (bio)chemical reaction. We have found that the viscoelastic nature of a crowded fluid (as quantified via the diffusion behavior of nanoparticles) can be varied without affecting the occupied-volume fraction by replacing solvents (MilliQ water vs TE buffer). Using this tunable crowded fluid, we observed that the number of open DNA hairpins, an experimental model for a simple on-off reaction, appears sensitive to crowding-induced viscoelasticity of the fluid. Using a simple statistical model, we were able to rationalize this experimental finding quantitatively. Comparing our results to previously published data on the formation of DNA double strands, it seems unlikely that a preferential interaction between crowders and our DNA hairpin was a major driving force. Based on our results, we suggest bearing in mind that macromolecular crowding may not be reduced to mere excluded-volume effects. Rather, viscoelasticity of the fluid and associated changes in the (re)binding rates need to be considered.

ACKNOWLEDGMENTS

We gratefully acknowledge Analytik Jena for providing the temperature-stabilized sample holder for the measurements reported in this study. O.S. acknowledges support by the Elite Network of Bavaria.

[1] J. R. Ellis and A. P. Minton, Nature (London) **425**, 27 (2003).
[2] H. X. Zhou, G. Rivas, and A. P. Minton, Annu. Rev. Biophys. **37**, 375 (2008).
[3] J. A. Dix and A. S. Verkman, Annu. Rev. Biophys. **37**, 247 (2008).
[4] M. Weiss, M. Elsner, F. Kartberg, and T. Nilsson, Biophys. J. **87**, 3518 (2004).
[5] I. M. Tolic-Nørrelykke, E.-L. Munteanu, G. Thon, L. Oddershede, and K. Berg-Sørensen, Phys. Rev. Lett. **93**, 078102 (2004).
[6] D. Banks and C. Fradin, Biophys. J. **89**, 2960 (2005).
[7] I. Golding and E. C. Cox, Phys. Rev. Lett. **96**, 098102 (2006).
[8] V. Tejedor, O. Bénichou, R. Voituriez, R. Jungmann, F. Simmel, C. Selhuber-Unkel, L. B. Oddershede, and R. Metzler, Biophys. J. **98**, 1364 (2010).
[9] S. C. Weber, A. J. Spakowitz, and J. A. Theriot, Phys. Rev. Lett. **104**, 238102 (2010).
[10] F. Hofling and T. Franosch, Rep. Prog. Phys. **76**, 046602 (2013).
[11] Y. He, S. Burov, R. Metzler, and E. Barkai, Phys. Rev. Lett. **101**, 058101 (2008).
[12] A. Lubelski, I. M. Sokolov, and J. Klafter, Phys. Rev. Lett. **100**, 250602 (2008).
[13] G. Guigas, C. Kalla, and M. Weiss, Biophys. J. **93**, 316 (2007).
[14] W. Pan, L. Filobelo, N. D. Q. Pham, O. Galkin, V. V. Uzunova, and P. G. Vekilov, Phys. Rev. Lett. **102**, 058101 (2009).
[15] J. Szymanski and M. Weiss, Phys. Rev. Lett. **103**, 038102 (2009).
[16] D. Ernst, M. Hellmann, J. Kohler, and M. Weiss, Soft Matter **8**, 4886 (2012).
[17] M. Weiss, Phys. Rev. E **88**, 010101(R) (2013).
[18] D. Ernst, J. Kohler, and M. Weiss, Phys. Chem. Chem. Phys. **16**, 7686 (2014).
[19] H. Berry, Biophys. J. **83**, 1891 (2002).
[20] M. Hellmann, D. Heermann, and M. Weiss, Europhys. Lett. **94**, 18002 (2011).
[21] M. Hellmann, D. Heermann, and M. Weiss, Europhys. Lett. **97**, 58004 (2012).
[22] O. Stiehl, K. Weidner-Hertrampf, and M. Weiss, New J. Phys. **15**, 113010 (2013).
[23] M. I. Wallace, L. Ying, S. Balasubramanian, and D. Klenerman, Proc. Natl. Acad. Sci. USA **98**, 5584 (2001).
[24] L. Xodo, G. Manzini, F. Quadrifoglio, G. van der Marel, and J. van Boom, Biochemistry **27**, 6327 (1988).
[25] T. G. Mason and D. A. Weitz, Phys. Rev. Lett. **74**, 1250 (1995).
[26] T. Gisler and D. Weitz, Curr. Opin. Colloid Interface Sci. **3**, 586 (1998).
[27] S. T. Hess and W. W. Webb, Biophys. J. **83**, 2300 (2002).
[28] A. P. Minton, Biopolymers **20**, 2093 (1981).
[29] T. C. Laurent, B. N. Preston, and B. Carlsson, Eur. J. Biochem. **43**, 231 (1974).
[30] S. B. Zimmerman, Biochim. Biophys. Acta **1216**, 175 (1993).
[31] D. B. Knowles, A. S. LaCroix, N. F. Deines, I. Shkel, and M. T. Jr. Record, Proc. Natl. Acad. Sci. USA **108**, 12699 (2011).